

~~RESTRICTED~~

UNCLASSIFIED

RM No. E8D13

21 JUL 1948

~~1201/1~~
~~134~~
~~1/1~~
C.1

NACA

RESEARCH MEMORANDUM

EXPERIMENTAL INVESTIGATION OF HOT-GAS BLEEDBACK FOR ICE

PROTECTION OF TURBOJET ENGINES

I - NACELLE WITH OFFSET AIR INLET

By Edmund E. Callaghan, Robert S. Ruggeri
and Richard P. Krebs

Flight Propulsion Research Laboratory
Cleveland, Ohio

CLASSIFICATION CANCELLED

Authority J. W. Crowley Date 12/14/53
EO 1.0.50/
By J. H. 1-11-54 See classification
RE 1987

This document contains classified information affecting the National Security of the United States within the meaning of the Espionage Act, USC 50-81 and 82. The transmission or the revelation of its contents in any manner to an unauthorized person is prohibited by law. Information so classified may be imparted only to persons in the military and naval services of the United States, appropriate civilian officers and employees of the Federal Government who have a legitimate interest therein, and to United States citizens of known loyalty and discretion who of necessity must be informed thereof.

TECHNICAL
EDITING
WAIVED

NATIONAL ADVISORY COMMITTEE FOR AERONAUTICS

WASHINGTON
July 9, 1948

UNCLASSIFIED

~~RESTRICTED~~

NACA LIBRARY
LANGLEY MEMORIAL AERONAUTICAL
LABORATORY
Langley Field, Va.

~~RESTRICTED~~

NACA RM No. ESD13

~~RESTRICTED~~



NATIONAL ADVISORY COMMITTEE FOR AERONAUTICS

RESEARCH MEMORANDUM

EXPERIMENTAL INVESTIGATION OF HOT-GAS BLEEDBACK FOR ICE

PROTECTION OF TURBOJET ENGINES

I - NACELLE WITH OFFSET AIR INLET

By Edmund E. Callaghan, Robert S. Ruggeri
and Richard P. Krebs

SUMMARY

Aerodynamic and icing investigations were conducted in the NACA Cleveland icing research tunnel on a two-thirds-scale model of a turbojet-engine nacelle in order to provide icing protection for the engine, protective screen, and accessory housing by the introduction of hot gases into the inlet-air stream.

An investigation of a hot-gas bleedback system consisting of a number of orifice holes peripherally located around the inlet opening was conducted for both dry-air and icing conditions. The temperature distribution in the model was determined as a function of hot-gas pressure and temperature for a single value of free-stream total temperature and a range of tunnel velocities.

Adequate ice protection was afforded when the minimum kinetic temperature in the protective screen was greater than 32° F. For an average air-temperature rise in the model of 40° F, the maximum deviation from the average was 8° F. The ram-pressure recovery of the inlet ducting for this condition was 77 percent.

INTRODUCTION

Experimental investigations show that the turbojet engine is vulnerable to impact icing. Even in a mild icing condition, the loss in air flow and the consequent increase in tail-pipe temperature usually prohibits continued operation. Some means of ice protection for the engine and inlet ducting is therefore necessary.

Three methods for such protection have been suggested. The most obvious of these methods is to keep those surfaces where ice may form

~~RESTRICTED~~

UNCLASSIFIED

at a temperature above the freezing point. Another method, inertia separation, has been experimentally investigated (references 1 to 3). The third method is to raise the temperature of the incoming air, by the introduction of hot gases, to a temperature that is sufficiently high to prevent the formation of ice. The third method is especially adaptable to a turbojet engine because the hot gas introduced into the inlet can be supplied by the engine. The hot gas may be obtained from either the turbine inlet or the tail pipe, and the 108s in thrust that each method involves has been analytically treated in an unpublished report. The results of this analysis show that an engine operating at rated rotational speed in an atmosphere of 0° F with 200-percent saturation can be protected from ice formations with a probable thrust loss of 5 to 17 percent. Because no ice accretions are permitted to form, normal engine operation may be achieved as soon as the airplane passes out of the icing condition.

The principal disadvantage of this method is that such an ice-protection system may complicate engine installations in which the cabin of the airplane is pressurized with air from the turbojet-engine compressor. Furthermore, if only sufficient gas is supplied for ice prevention (prohibition of ice accretion), the system will probably be ineffective as a de-icer (removal of ice already formed).

An investigation of a two-thirds-scale model of a jet-engine nacelle was conducted in the NACA Cleveland icing research tunnel. The nacelle represented one-half of a two-engine nacelle similar to that employed in a four engine jet bomber of 91,000 pounds gross weight. The model was provided with holes for introducing hot gas into the inlet. Data were obtained to determine the effect of gas temperature and pressure, tunnel velocity, and angle of attack on the temperature distribution at the simulated engine inlet. The icing investigation to determine the minimum heat requirements was conducted over a range of liquid-water contents from 0.3 to 1.1 grams per cubic meter and at a total temperature of 0° F with the model at an angle of attack of Co.

APPARATUS

Description of model. - The nacelle investigated represents one duct of a twin nacelle housing two turbojet engines and a main landing wheel. The model is two-thirds of full scale, constructed of steel, Inconel, and aluminum, and has an inlet area of 1.24 square feet; it was designed for a maximum airflow of 32 pounds per second. For convenience in changing angle of attack, the inlet and the duct were rotated 90° about the longitudinal axis from the normal installation in the aircraft. The model as installed in the test section

of the tunnel and a typical airplane installation are shown in figure 1.

A 1/4-inch mesh, 0.050-inch-diameter wire screen was mounted in the model, as shown in figures 1 and 2, to simulate a typical protective screen installation. Air flow through the model and inlet-velocity ratios were controlled by an electrically driven tail cone (fig. 2).

Description of hot-gas bleedback system. - A sketch of a part of the hot-gas ducting, the plenum chamber in the nose, and the orifice holes is shown in figure 1. The hot gas was obtained by passing high-pressure air through a combustion heater and by ducting the air to the model.

The location and diameter of the orifice holes in the model were chosen in accordance with the results reported in reference 5. In order to obtain the maximum penetration, the jets were located as far upstream of the simulated engine as possible, that is, at the model inlet. The section of the inlet at the lip was used as plenum chamber for the hot gas, which also afforded icing protection for the lip.

The orifice configuration investigated consisted of six 1/2-inch-diameter holes and ten 3/8-inch-diameter holes, spaced as shown in figure 3, and located in a plane approximately 6 inches back of the leading edge of the nacelle lip, as shown in figure 2.

INSTRUMENTATION

The model instrumentation used in the investigation is shown in figure 2. The four front pressure rakes shown in figure 2 were located 90° apart and contained six total-pressure tubes and one static-pressure tube. Static pressures were also measured ahead of and behind the screen by two groups of four static-pressure tubes located 90° apart. The four rear rakes were offset 5° from the front rakes and consisted of five total-pressure tubes and one static-pressure tube. All pressure tubes were electrically heated to prevent the formation of ice accretions.

The average air temperature and temperature distribution inside the model were measured by means of a thermocouple cross rake mounted in the duct 43 inches downstream of the orifice holes and just ahead of the simulated accessory housing, as shown in figure 2. The rake consisted of 29 total-temperature thermocouples spaced 1 inch apart and mounted in two streamlined struts intersecting at 90°.

Temperatures on the duot surface were measured by 47 flush-type thermocouples, of which 30 were mounted on the duot outer wall and 17 were mounted on the accessory housing. Temperatures directly ahead of the screen were measured by two thermocouples located on each support strut and temperatures behind the screen in the plane of the rear pressure rakes were measured by four thermocouple probes.

The state of the gas in the plenum chamber was measured by four thermocouples located 90° apart in the plane of the orifice hole and by four static-pressure tubes located in the rear wall of the plenum chamber. Gas flow through the orifice holes was measured by an orifice located in the ducting between the combustion chamber and the model.

All pressure data were photographically recorded from multiple manometers and the temperature data were automatically recorded by use of flight recorders.

SYMBOLS

The following symbols are used in this report:

c_p	specific heat of air, (Btu/(lb)(°F))
$c_{p,g}$	specific heat of gas, (Btu/(lb)(°F))
P_f	total pressure inside model, (lb/sq ft)
P_0	free-stream total pressure, (lb/sq ft)
Δp	static-pressure drop across screen, (lb/sq ft)
q	dynamic pressure ahead of screen, (lb/sq ft)
q_0	free-stream dynamic pressure, (lb/sq ft)
T_{av}	arithmetic average total temperature in model, (°F)
T_g	calculated hot-gas total temperature, (°F)
T_0	free-stream total temperature, (°F)
W_a	airflow through model, (lb/sec)
W_g	hot-gas flow through orifice holes, (lb/sec)
η	ram-pressure recovery, $1 - \left(\frac{P_0 - P_f}{q_0} \right)$

PROCEDURE

Aerodynamic investigation without bleedback. - An aerodynamic investigation of the model without Orifice holes was conducted to determine air-flow characteristics and ram-pressure recovery as a function of inlet velocity ratio and angle of attack for a range of tunnel velocities from 200 to 400 feet per second. At each tunnel velocity investigated, the angle of attack was varied from 0° to 8° and for each angle of attack the inlet velocity ratio was varied from 0.40 to 0.62.

Aerodynamic investigation with bleedback. - A number of orifice configurations were investigated in order to obtain a configuration that would give a uniform temperature distribution inside the model for a range of values of tunnel velocity, angle of attack, gas flow, and gas temperature. The configuration chosen is shown in figure 3.

The effect of hot-gas bleedback on the temperature distribution inside the model, air-flow characteristics, and ram-pressure recovery for the optimum orifice configuration was determined for the same range of values of tunnel velocity and angle of attack as used in the aerodynamic investigation without hot-gas bleedback. In addition, the investigation was also conducted with 8 fixed tail-cone position corresponding to a velocity ratio of 0.62 without bleedback. The range of gas flows and plenum-chamber gas temperatures was from 0.4 to 1.4 pounds per second and from 600° to 1200° F, respectively. For each plenum-chamber gas temperature, the gas pressure was varied from 3000 to 6000 pounds per square foot absolute.

In order to determine the reduction in ram-pressure recovery due to the jet penetration alone, cold gas was bled into the model at pressures up to 3000 pounds per square foot absolute at several tunnel velocities and at an angle of attack of 0°.

Icing with bleedback. - An investigation to determine the critical icing criterion as a function of the mass air flow, gas flow, gas temperature, and liquid-water content for a constant free-stream total temperature of 0° was conducted in the following manner:

For a constant tunnel velocity, an excess of hot gas was introduced into the model to insure adequate ice protection. After sufficient time had elapsed for conditions to stabilize, liquid water was introduced into the air stream. A 5-minute time interval was selected to observe if any ice accretion occurred as evidenced by a noticeable reduction of air flow. If no noticeable reduction in air flow occurred, the plenum-chamber gas pressure was reduced 350 pounds

per square foot and another 5-minute observation period was held. This process was repeated until ice had formed and air flow had appreciably reduced.

Pressure data were recorded at the beginning and the end of each time interval and temperature data were continuously recorded. This investigation was conducted at tunnel velocities of 200, 290, 355, and 415 feet per second with liquid-water content from 0.3 to 1.1 gm. w per cubic meter at an average drop diameter of 15 microns. The plenum-chamber gas-temperature ranged from 700° to 1100° F.

Plenum-chamber gas-temperature correction. - During the investigation, the plenum-chamber gas-temperature readings were consistently low because of thermocouple radiation effects. Calibration of the plenum-chamber thermocouples by utilizing the following heat-balance equation was therefore necessary:

$$c_p (W_g - W_0) (T_{av} - T_0) = W_g (T_g - T_{av}) c_{p,g}$$

A curve showing the relation between the measured and calculated plenum-chamber temperatures is shown in figure 4. For all subsequent calculations involving plenum-chamber gas temperature, the corrected value was used.

RESULTS AND DISCUSSION

Aerodynamic Investigation without Bleedback

Ram-pressure recovery. - A ram-pressure recovery η of about 0.99 was obtained at an angle of attack of 0° and an inlet velocity ratio of 0.82. A very slight decrease in ram-pressure recovery was observed with decreasing inlet velocity ratio and increasing angle of attack.

Mass-flow characteristics. - The mass flow through the model varied linearly with tunnel velocity for fixed tail-cone position and angle of attack. A maximum flow of approximately 31 pounds per second was obtained at an inlet velocity ratio of 0.82, 8 tunnel velocity of 430 feet per second, and an angle of attack of 0°.

Aerodynamic Investigation with Bleedback

Air-temperature distribution. - 5 data presented in this report are for 8 single jet configuration that is considered optimum in regard

to uniform temperature distribution. Uniform distribution was obtainable at only a few combinations of hot-gas plenum-chamber pressure and temperature, tunnel velocity, and angle of attack. The most uniform temperature distribution occurred when the plenum-chamber gas temperature and pressure were 965° F and 4560 pounds per square foot, respectively, at 8 tunnel velocity of 290 feet per second and an angle of attack of 0°. Under these conditions, the temperature inside the model was raised from a total temperature of 0° F to an average total temperature of 45.7° F and the maximum deviation from the average was 6° F.

The effect of plenum-chamber gas pressure on the temperature distribution at the thermocouple cross rake is illustrated in figure 5. In this and subsequent figures, lines of constant total-temperature rise above free-stream total temperature are indicated. The figures representing the temperature-rise distribution at the thermocouple cross rake are in the position in which the model was mounted in the tunnel. The four distributions were taken at 8 tunnel velocity of 290 feet per second, 8 plenum-chamber total gas temperature of approximately 915° F, and an angle of attack of 0°. At the lowest plenum-chamber gas pressure (4000 lb/sq ft), a high temperature region existed to the left and above the center (fig. 5(a)) and a rather severe gradient existed in the upper right sector. Increasing the pressure to 4700 pounds per square foot (fig. 5(b)) eliminated the high-temperature island and decreased the temperature extremes, but a further increase in the plenum-chamber pressure to 5500 or 6300 pounds per square foot (figs. 5(c) and 5(d)) again increased the temperature extremes. Because the jets in the nose of the model are fixed in size, the plenum-chamber gas pressure could not be increased without increasing the gas flow. Higher temperatures were therefore encountered in the model with increased gas pressure for 8 constant plenum-chamber gas temperature. As the average temperature rise was increased, there was an accompanying increase in temperature gradient.

An increase in the plenum-chamber temperature increased the temperature rise in the model (fig. 6), but had little effect on the temperature extremes or the temperature distribution pattern. All data presented in figure 6 were obtained at 8 tunnel velocity of 290 feet per second, a plenum-chamber pressure of 5500 pounds per square foot, and an angle of attack of 0°.

Increasing the tunnel velocity increased both the air flow through the model and the inlet velocity. A 5 increase in air flow lowered the average air-temperature rise in the model for constant values of 811 other variables. A 5 increase in inlet velocity had

8 decided effect on the temperature-rise distribution inside the model, 88 illustrated in figure 7. The temperature-rise contours are for nearly constant manifold conditions, a plenum-chamber gas temperature of 1145° F, 8 plenum-chamber gas pressure of 5500 pounds per square foot, and an angle of attack of 0°.

Changing the angle of attack of the model from 0° to 8° had no effect on the temperature rise in the model (fig. 8). The similarity of isotherm lines is illustrated for the following condition: tunnel velocity, 200 feet per second; plenum-chamber gas temperature, 1210° F; plenum-chamber gas pressure, 5500 pounds per square foot.

Skin temperatures. - The highest skin temperature measured was 125° F and was obtained at 8 point adjacent to the hot-gas ducting. In addition, the average air total temperature inside the model was approximately 80° F. For an average air total temperature of approximately 40° F, the skin temperature did not exceed 100° F.

Mass flow and ram-pressure recovery losses due to bleedback. - The hot-gas jets reduced the air flow as the temperature in the model increased. The decrease in air flow with temperature for several values of tunnel velocity and an angle of attack of 0° is shown in figure 9. If these curves were extrapolated to a model temperature of 0° F corresponding to the tunnel temperature of 0° F, the resultant mass air flow would be the same as that obtained without jets. The decrease in air flow through the model when the jets are turned on is primarily caused by the change in density of the air and secondarily by the momentum pressure loss associated with adding heat to 8 moving stream.

Ram-pressure recovery is adversely affected by the presence of the jets. When the model was first investigated without orifice holes, 8 ram-pressure recovery of approximately 0.99 was realized. Subsequent warping of the model, caused by high manifold pressures and temperatures, and the installation of orifice holes reduced the ram-pressure recovery without the jets to about 0.91. The introduction of cold gas under pressure through the orifice holes reduced the ram-pressure recovery another 5 to 6 percent. 5 effect on ram-pressure recovery of raising the temperature in the model by means of hot-gas jets is shown in figure 10. A part of the reduction in ram-pressure recovery can be attributed to the loss in total pressure associated with the addition of heat. 5 remainder of the loss is due to the loss of total pressure arising from the mixing of the jets with the air flow through the model. Ram-pressure recovery is believed to decrease slightly with increasing plenum-chamber pressures and decreasing tunnel velocity, but the effects are obscured by the spread of the data.

Icing with Bleedback

In analyzing the icing data, the pressure-drop coefficient $\Delta p/q$ across the inlet screen was computed for each icing run. The screen was considered iced when the value of $\Delta p/q$ approached approximately 1.5 times the value for the screen at the beginning of each run. The percent bleedback W_g/W_a and plenum-chamber gas temperature corresponding to this criterion are plotted in figure 11 for tunnel velocities of 290 and 355 feet per second. No ice accretions were observed on the accessory housing and nacelle lip when the inlet screen was iced.

Three theoretical curves shown in figure 11 are based on the following analysis: Icing on the screen was assumed to occur when the minimum kinetic temperature (static temperature plus 0.85 times the dynamic temperature rise) on the screen was 32° F. From the data taken without sprays, when the average air temperature in the model was determined to be approximately 40° F, the temperature deviation at the cross rake was approximately 8° . Under these conditions, the ram-pressure recovery (fig. 10) was 77 percent. In order to maintain a minimum kinetic temperature in the screen of 32° F, an average total temperature of 41.4° inside the model was necessary with a velocity in the screen of 350 feet per second corresponding to a tunnel speed of 290 feet per second. The theoretical curve A in figure 11 related the gas temperature and percent bleedback required to maintain a total temperature of 41.4° F in the model with a tunnel velocity of 290 feet per second, a tunnel temperature of 0° F, and dry air.

Curve B in figure 11 was calculated for the same temperature inside the model for a wet-air condition. The amount of moisture in the air used to compute this curve was assumed to be about the maximum possible water content in the tunnel at 290 feet per second and 0° F with the sprays on, and was assumed to consist of the water in 200-percent saturated air at 0° F plus a liquid-water content of 1 gram per cubic meter. Curve C was calculated for the same water content and kinetic temperature in the screen, but at a tunnel velocity of 355 feet per second corresponding to a screen velocity of 430 feet per second. The total air temperature in the model required for ice prevention under these conditions was 42.3° F.

An examination of figure 11 shows that most of the data falls within the limits of the three curves. The correlation of data and theory indicates that icing will not occur if the surface kinetic temperature is maintained above freezing. If all the conditions of the investigation had been ideal, all the lower speed data would

have fallen between curves A and B and all the higher speed data would have been to the left of curve C. Actually, the displacement of some of the data points to higher than theoretical amounts of bleedback is attributable to several factors: the nonuniformity of liquid water in the model, the variation of screen solidity, and the velocity distribution ahead of the screen.

SUMMARY OF RESULTS

The following results were obtained from an icing-research-tunnel investigation of a two-thirds-scale nacelle for 8 turbojet-engine nacelle. The nacelle was provided with orifice holes for admitting hot gas to the engine-inlet duct for ice prevention.

1. The inlet screen of the model was kept practically free of ice, provided sufficient hot gas was supplied to keep the kinetic temperature throughout the screen above 320 F.

2. For 8 dry-air condition, the maximum deviation from the average air-temperature rise at the simulated engine inlet was about 8° F for an average air-temperature rise in the model of 400 F. The addition of heat required for 8 40° F air-temperature rise lowered the ram-pressure recovery to about 77 percent.

3. Changes in duct-inlet velocity greatly affected the temperature distribution inside the model. More uniform temperature distributions were obtained at high plenum-chamber gas pressures. Changes in hot-gas temperature and angle of attack had little effect on the temperature-distribution pattern.

4. The introduction of cold gas under pressure through the orifice holes decreased the ram-pressure recovery in the model by 5 to 6 percent.

5. The decrease in mass flow with hot-gas bleedback was almost entirely attributable to the decrease of the air density resulting from the increase in air temperature in the model..

Flight Propulsion Research Laboratory,
National Advisory Committee for Aeronautics,
Cleveland, Ohio.

REFERENCES

1. von Glahn, Uwe: Ice Protection of Turbojet Engines by Inertia Separation of Water. I - Alternate-Duct System. NACA RM No. E8A27, 1948.
2. von Glahn, Uwe: Ice Protection of Turbojet Engines by Inertia Separation of Water. II - Single-Offset-Duct System. NACA RM No. E8A28, 1948.
3. von Glahn, Uwe: Ice Protection of Turbojet Engines by Inertia Separation of Water. III - Annular Submerged Inlets. NACA RM No. E8A29, 1948.
4. Callaghan, Edmund E., and Ruggeri, Robert S.: Investigation of the Penetration of an Air Jet Directed Perpendicularly to an Air Stream. NACA TN No. 1615, 1948.

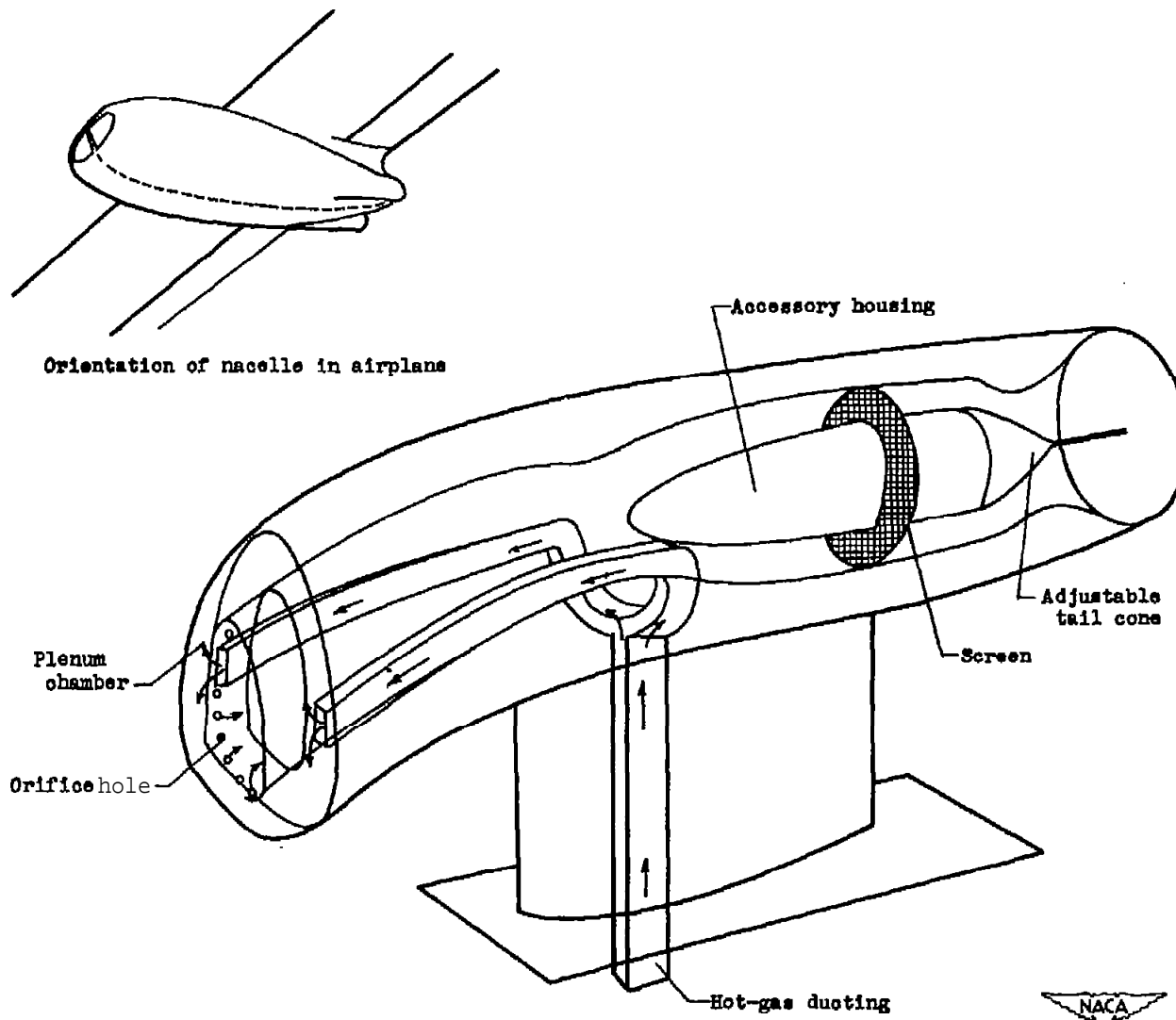


Figure 1. - Sketch showing hot-ma ducting and model installation in tunnel test section.

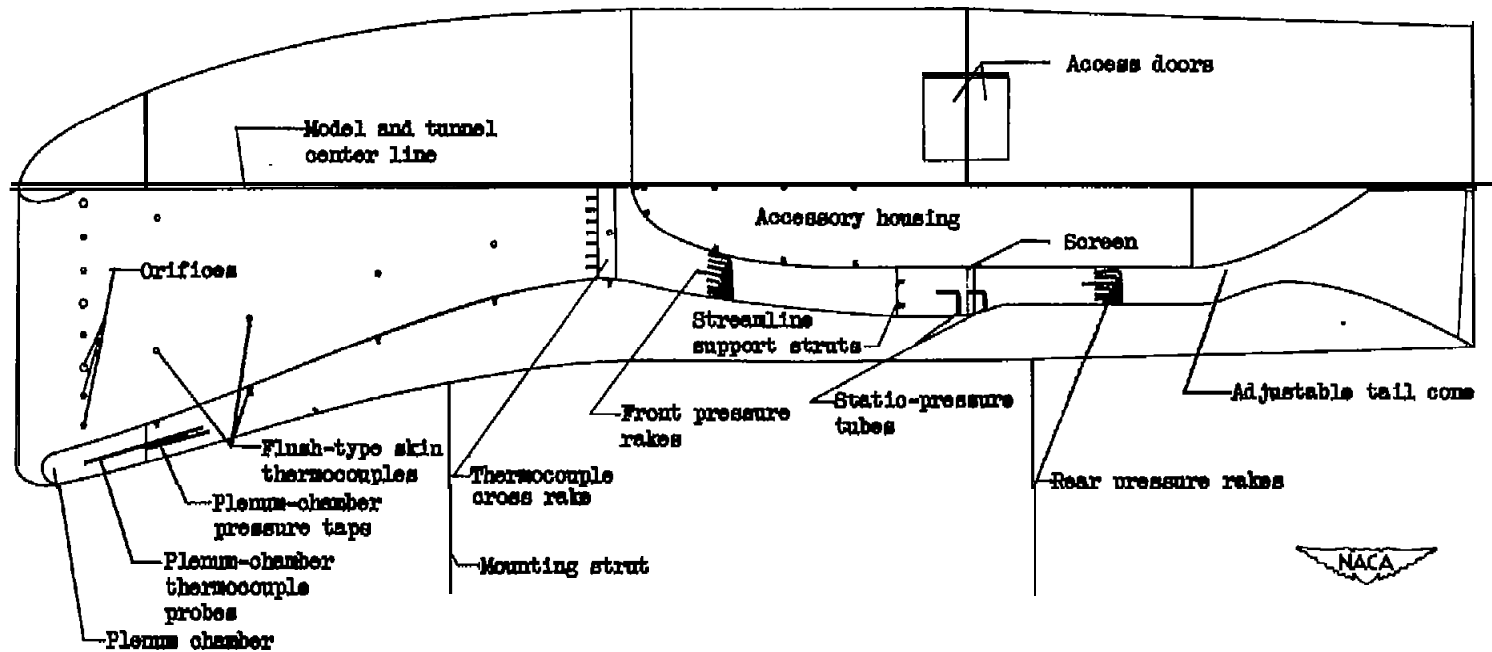


Figure 2. - Location of instrumentation on model of turbojet-engine nacelle.

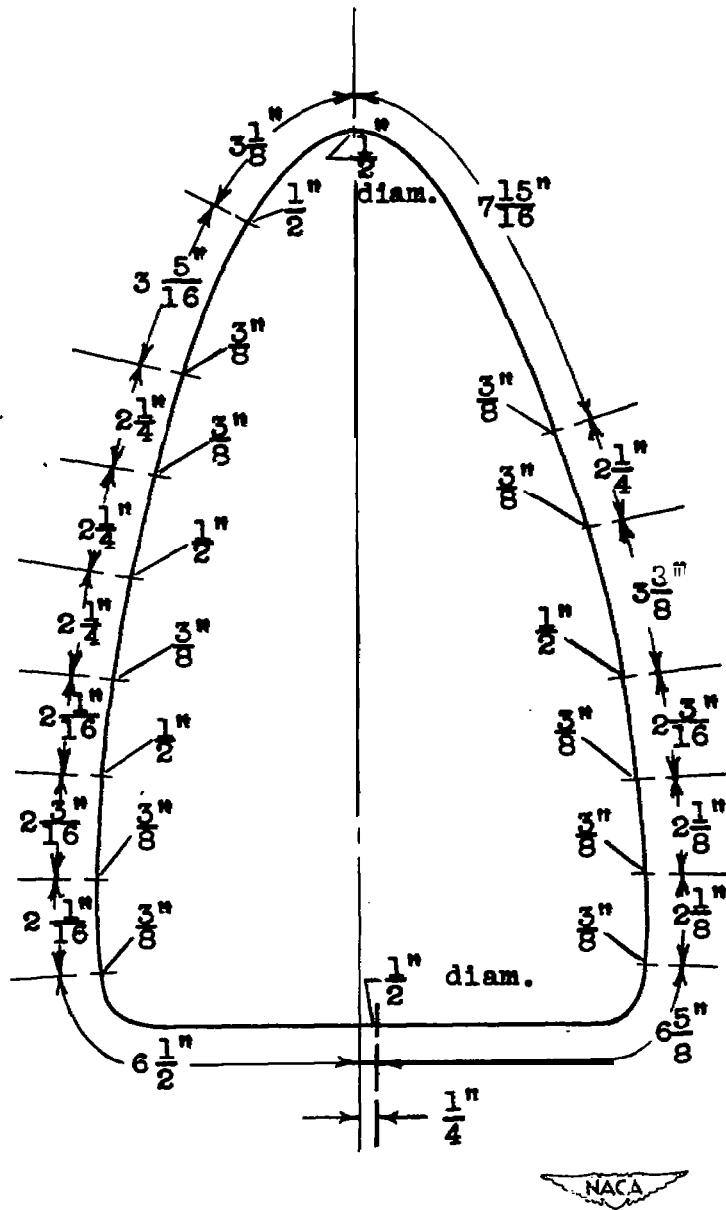


Figure 3. - Sketch showing **location** and **size** of orifice holes for optimum orifice configuration.

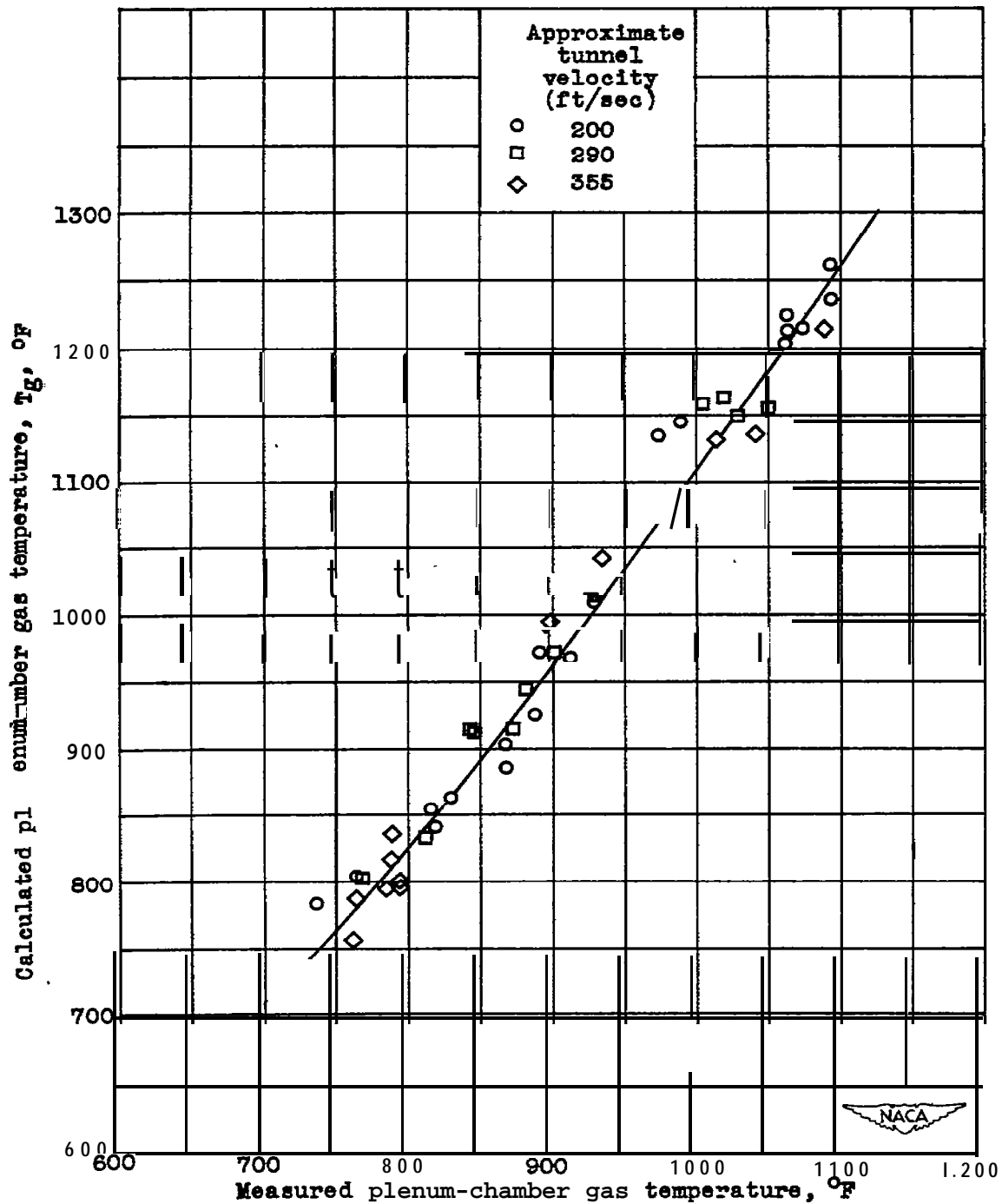


Figure 4. - Relation between calculate& and measured plenum-chamber gas temperatures.

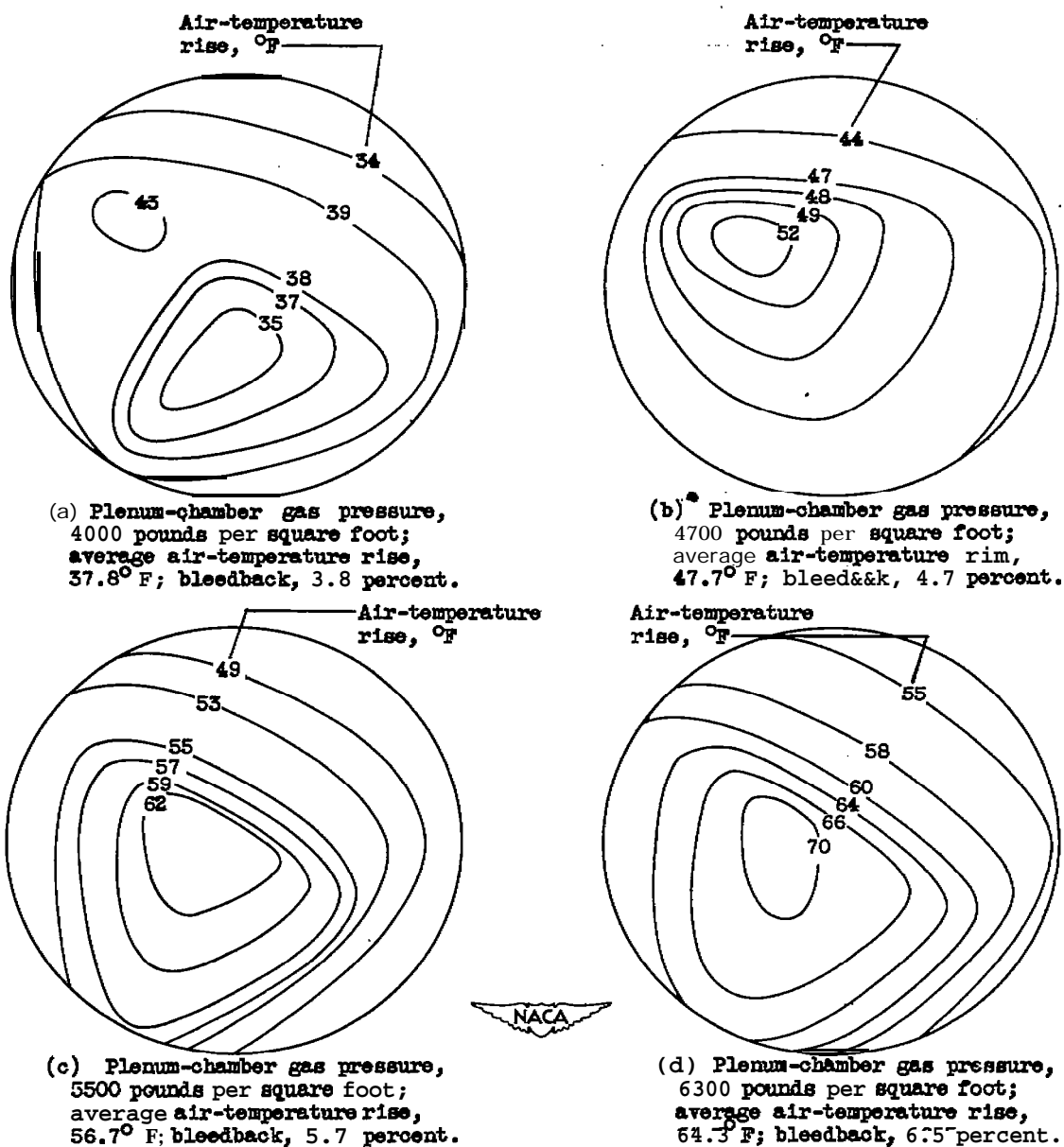


Figure 5. - Effect of plenum-chamber gas pressure on air-temperature rise distribution at thermocouple cross rakes. Tunnel velocity, 290 feet per second; plenum-chamber gas temperature, 915° F; angle of attack, 0°.

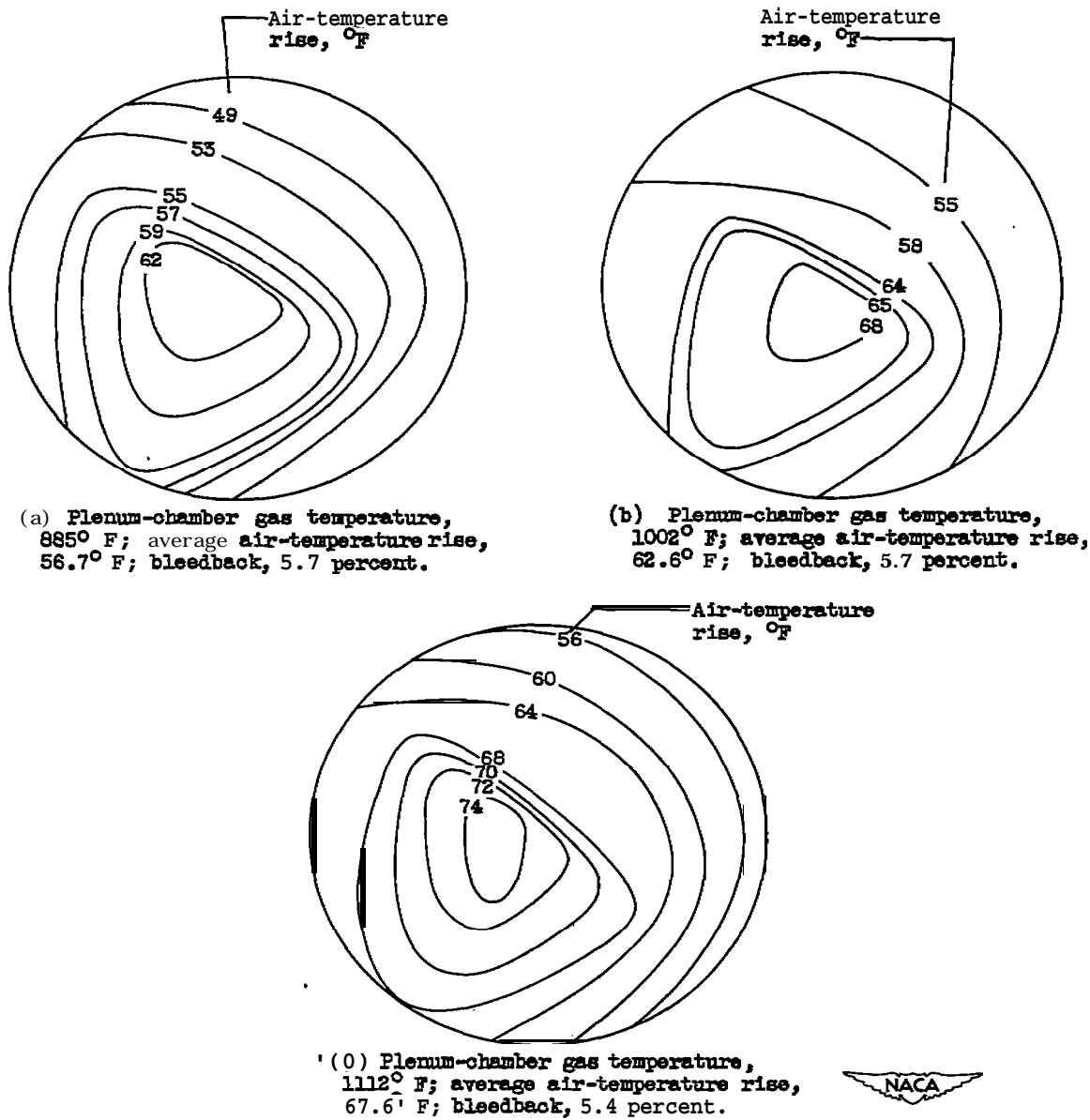
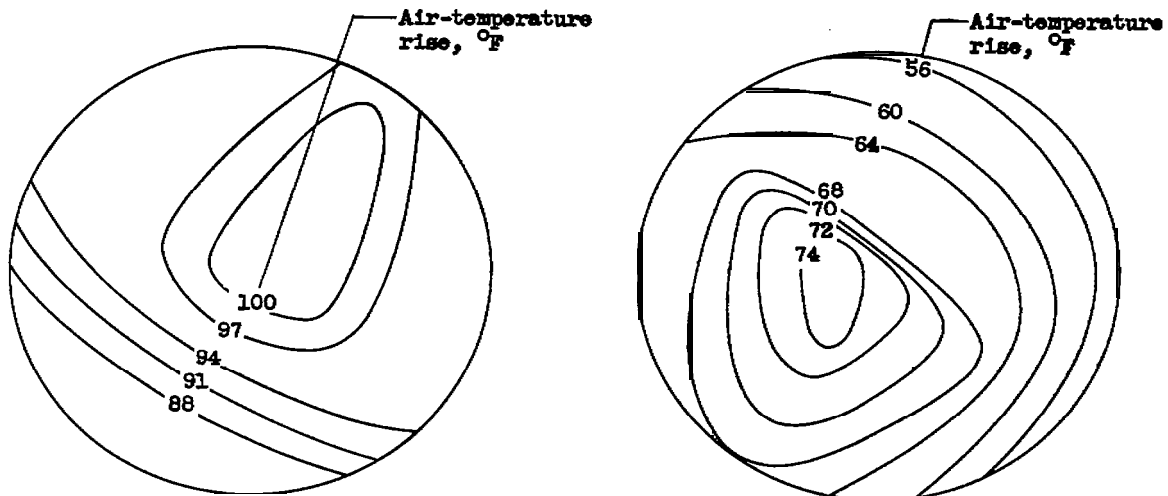
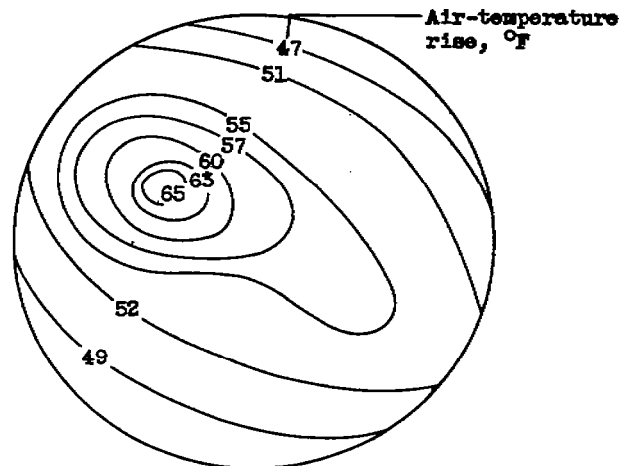


Figure 6. - Effect of plenum-chamber gas temperature on air-temperature rise distribution at thermocouple cross rake. Tunnel velocity, 290 feet per second; plenum-chamber gas pressure, 5500 pounds per square foot; angle of attack, 0°.



(a) Tunnel velocity, 220 feet per second; average air-temperature rise, 97.8°F; bleedback, 8.0 percent.

(b) Tunnel velocity, 290 feet per second; average air-temperature rise, 67.8°F; bleedback, 5.4 percent.

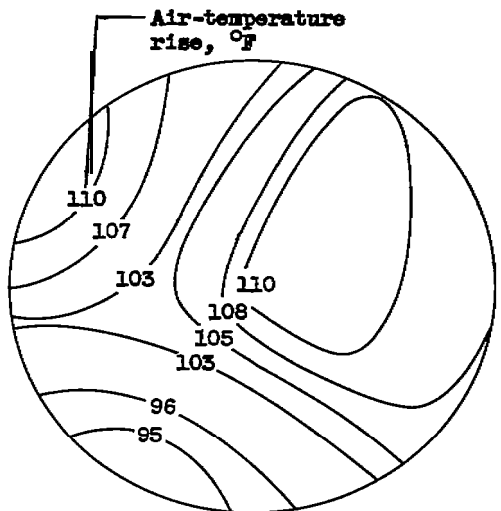


(c) Tunnel velocity, 415 feet per second; average air-temperature rise, 54.9°F; bleedback, 4.4 percent

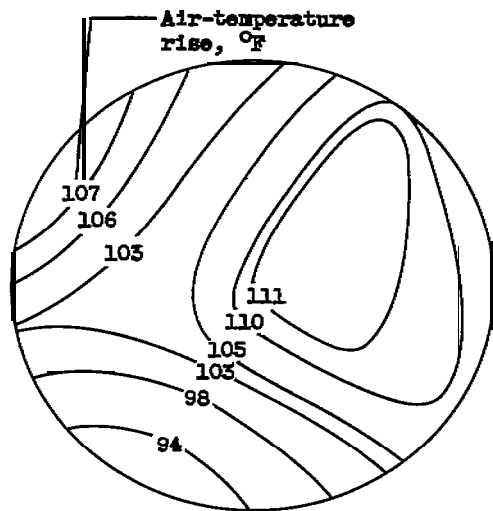


Figure 7. - Effect of tunnel velocity on air-temperature rise distribution at thermocouple cross rake. Plenum-chamber gas temperature, 1145°F; plenum-chamber gas pressure, 5500 pounds per square foot; angle of attack, 0°.

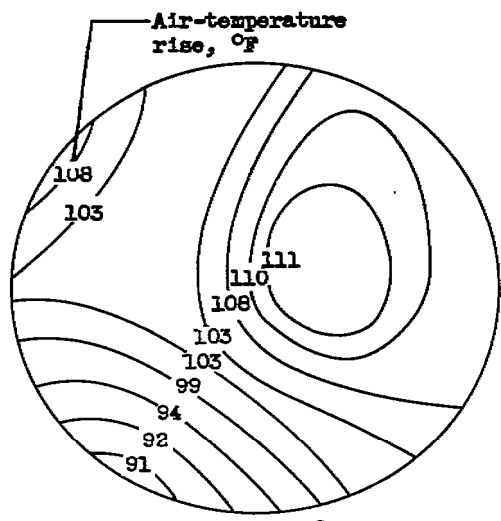
960



(a) Angle of attack, 0° ; average air-temperature rise, 107.2° F .



(b) Angle of attack, 4° ; average air-temperature rise, 107.1° F .



(c) Angle of attack, 8° ; average air-temperature rise, 106.2° F .



Figure 8. - Effect of angle of attack on air-temperature rise distribution at thermocouple cross rake. Tunnel velocity, 200 feet per second; plenum-chamber gas temperature, 1210° F ; plenum-chamber gas pressure, 5500 pounds per square foot; bleedback, 8.2 per cent.

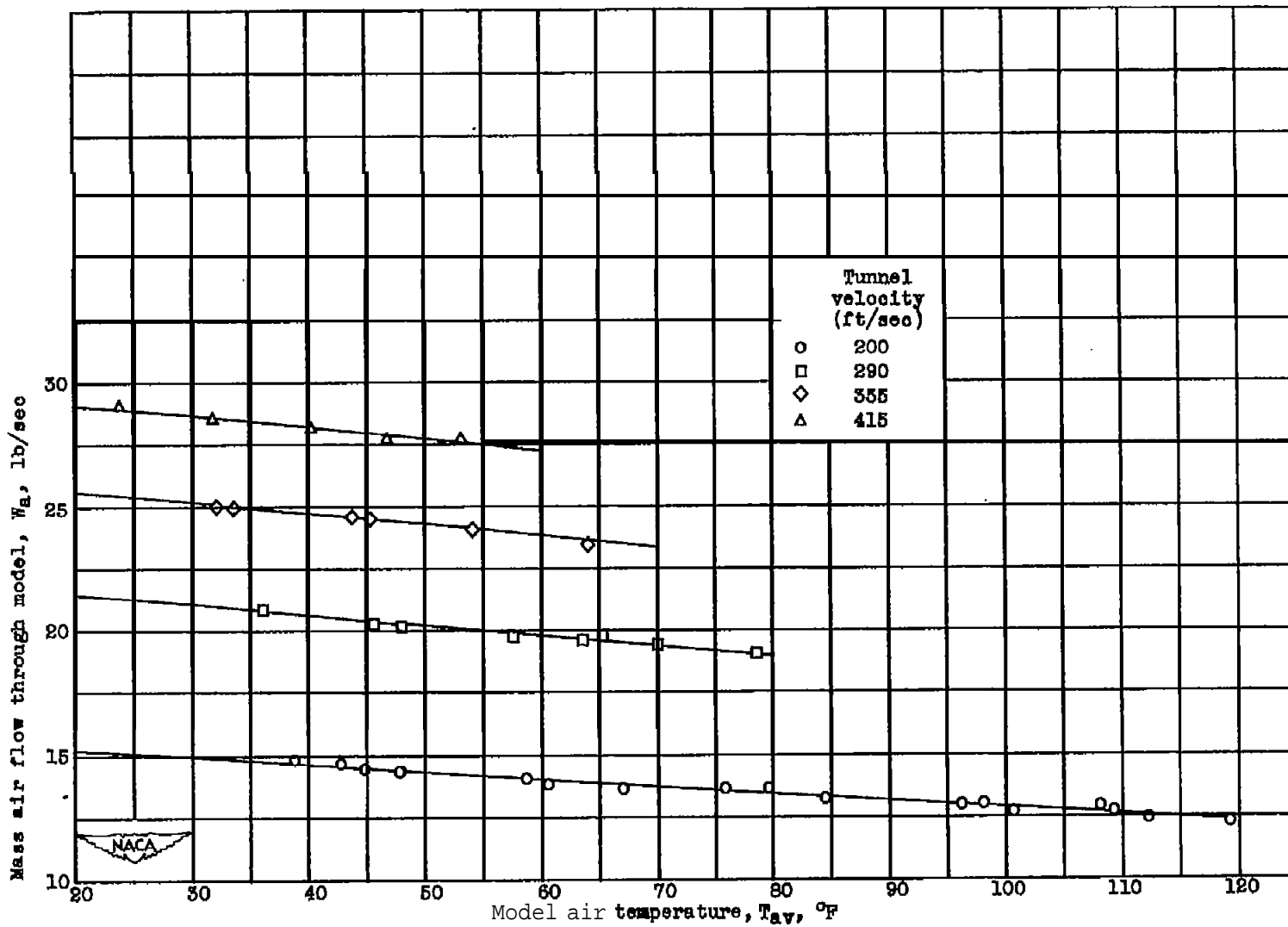


Figure 9. - Variation of mass air flow through model with model air temperature for various tunnel velocities. Angle of attack, 0° ; tunnel total temperature, 0° F.

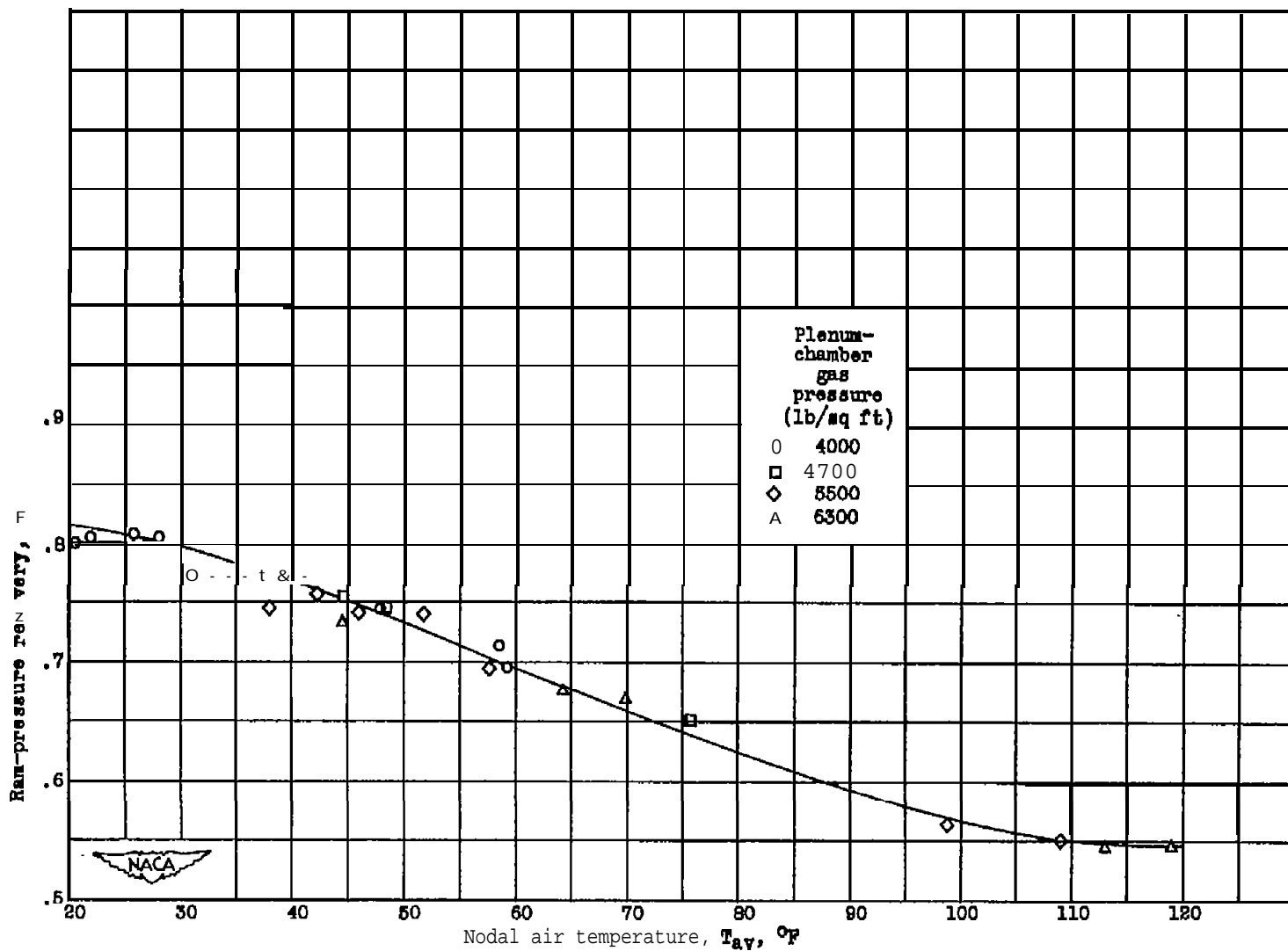
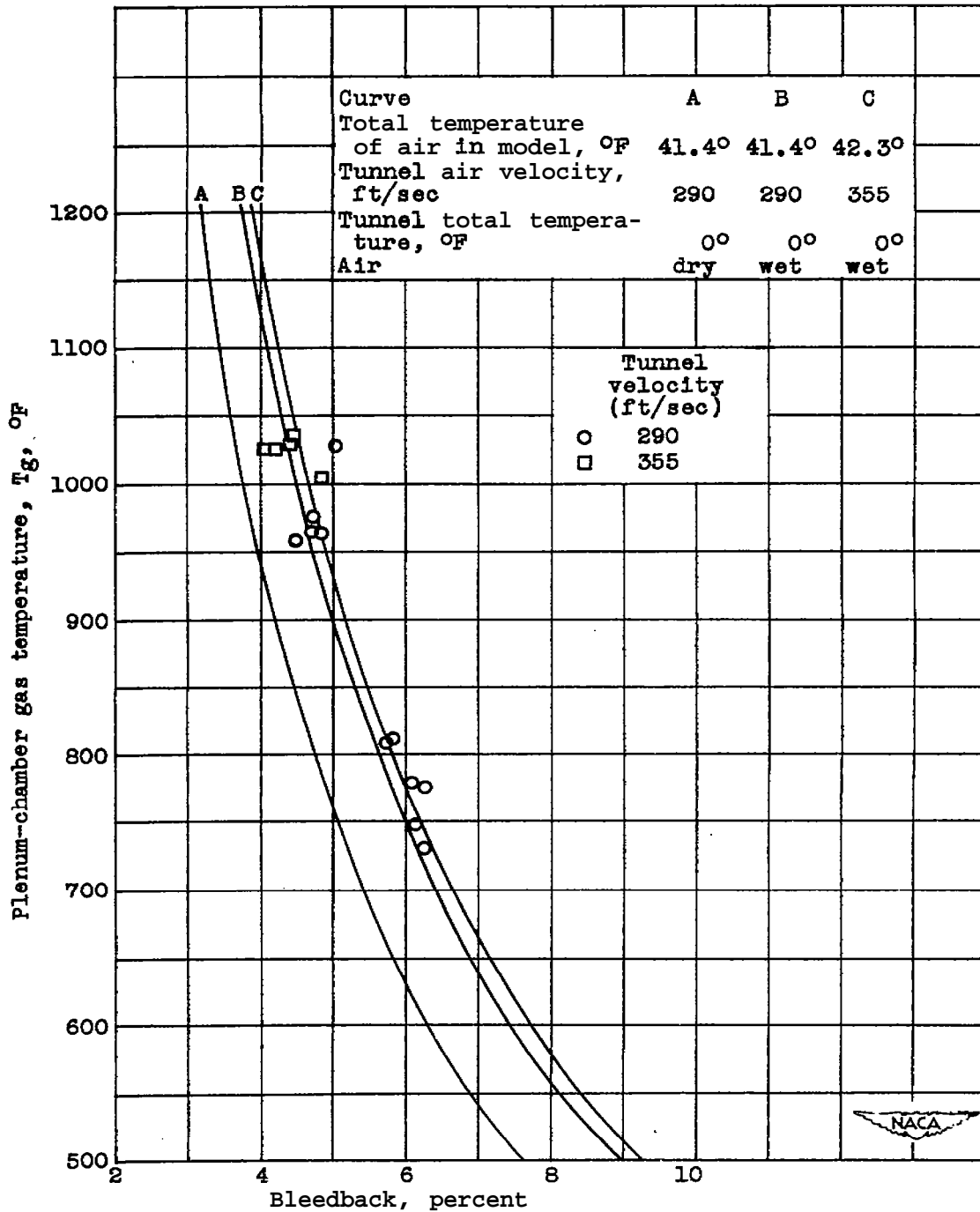


Figure 10. - Variation of ram-pressure recovery with model air temperature. Angle of \bullet ttrok, 0° ; tunnel total temperature, 0° F.



096

Figure 11. - Bleedback required for ice prevention as function of plenum-chamber gas temperature for free-stream total temperature of 0° F.

NASA Technical Library



3 1176 01435 5219



1

1